Highly conductive p^{++}-AlGaAs/n^{++}-GaInP tunnel junctions for ultra-high concentrator solar cells

Enrique Barrigón , Ivan García , Laura Barrutia , Ignacio Rey-Stolle and Carlos Algora

ABSTRACT

Tunnel junctions are key for developing multijunction solar cells (MJSC) for ultra-high concentration applications. We have developed a highly conductive, high bandgap p^{++}-AlGaAs/n^{++}-GaInP tunnel junction with a peak tunneling current density for as-grown and thermal annealed devices of 996 A/cm^2 and 235 A/cm^2, respectively. The J–V characteristics of the tunnel junction after thermal annealing, together with its behavior at MJSCs typical operation temperatures, indicate that this tunnel junction is a suitable candidate for ultra-high concentrator MJSC designs. The benefits of the optical transparency are also assessed for a lattice-matched GaInP/GaInAs/Ge triple junction solar cell, yielding a current density increase in the middle cell of 0.506 mA/cm^2 with respect to previous designs. Copyright © 2014 John Wiley & Sons, Ltd.

KEYWORDS

tunnel junction; multijunction solar cell; concentrated photovoltaics; AlGaAs; GaInP

1. INTRODUCTION

In recent years, several types of multijunction solar cells (MJSC) have shown efficiencies in excess of 40% under concentrated light [1–5] and recent studies predict efficiencies close to 50% for MJSCs with more than three junctions [6]. In the quest for producing cost-competitive electricity from concentrator photovoltaics (CPV), not only high cell efficiencies are needed, but also efficient operation of the MJSCs at ultra-high concentration (beyond 1000 suns) should be accomplished [7]. Consequently, the design of high-efficiency MJSCs to work under ultra-high concentration also demands the minimization of electrical and optical losses in the parts of the device that are not directly involved in the photovoltaic conversion, such as the tunnel junctions (TJ).

A monolithic MJSC consists of a stack of different subcells, each one having a different energy bandgap, and are electrically connected by tunnel junctions. A TJ is a thin highly doped p–n junction [8] that connects the p-side of one subcell to the n-side of the adjacent subcell. TJs in the field of MJSCs are characterized by two main figures of merit, namely, the peak tunneling current (J_p) and the equivalent resistance (r_s). For ultra-high concentration applications, TJs should show sufficiently low r_s and high J_p so that the performance of the solar cell is not compromised by the TJ. The equivalent resistance should be as low as possible to avoid being the limiting vertical component in the series resistance of the device [9]. Besides, a high peak tunneling current is desirable to

- be well above the photocurrent generated by the solar cell under concentration;
- withstand peak irradiances on the cell arising from non-uniform illumination profiles created by the optics of CPV modules [10]; and
- increase the margin for the eventual degradation of their performance after the thermal load originated during the growth of subsequent subcells in a MJSC stack [11,12].

In this way, the TJ is forced to work at the ohmic region of its J–V curve and will cause a voltage drop directly related to the value of r_s. From an optical standpoint, TJs should likewise present a high optical transmittance (by the use of high bandgap materials) so that the absorption of photons potentially absorbable by lower subcells is minimized. However, high peak tunneling currents are in principle

obtained with low bandgap materials [8], which diminishes the optical transparency of the TJ. As a result, a trade-off between high optical transparency and high peak tunneling current must be solved in order to achieve solar cells with high efficiency at ultra-high concentrations.

In a previous work [13], we presented the highest J_p reported to date (10 100 A/cm^2) for a TJ device in the field of III–V MJSCs lattice matched to any of the typical substrates (GaAs or Ge). That design was based on a p^{++}-AlGaAs:C/n^{++}-GaAs:Te heterostructure lattice-matched to GaAs, which had a non-negligible optical absorption if used between a GaInP and a GaAs solar cell. Thus, in order to improve the transparency of the TJ, the GaAs-based cathode should be replaced by a material with a higher bandgap, at possibly the expense of a reduction in J_p. Theoretically, the use of an n-type AlGaAs cathode should solve the problem, but the achievement of a reproducible n-type AlGaAs doped to degeneracy has demonstrated to be elusive [14]. An alternative design based on heterojunctions was proposed by Jung *et al.*[11], who published the first p^{++}-AlGaAs:C/n^{++}-GaInP:Se TJ grown by atomic layer epitaxy. This device exhibited a J_p of 83 A/cm^2, but this value dropped to 74 and 33 A/cm^2 once annealed for 30 min at 650 °C and 750 °C, respectively. *J–V* curves of tunnel diodes for MJSCs grown by MOVPE based on the same heterostructure were presented with J_p values of 50 A/cm^2 [15], 80 A/cm^2 [16], and 637 A/cm^2 [17]. The effect of the thermal load in the *J–V* curve was neither shown nor mentioned in any of these works.

In this paper, we present a p^{++}-AlGaAs:C/n^{++}-GaInP:Te tunnel junction with a measured peak current of 996 A/cm^2 and an equivalent resistance of 7×10^{-5} $\Omega\cdot$ cm^2. After thermal annealing emulating the top cell growth (see below for the experimental details), the devices showed a drop of J_p to 235 A/cm^2, which corresponds to a concentration of about 15 600 suns, assuming a one-sun short-circuit current density (J_{sc}^{1X}) of $\sim$ 15 mA/cm^2. The equivalent resistance showed an increase to 1.4×10^{-4} $\Omega\cdot$ cm^2, although it satisfies the requirements for its implementation in MJSCs designed to work under ultra-high concentrations. The benefits of the optical transparency of the TJ for a conventional design grown on a Ge substrate are also shown.

2. EXPERIMENTAL

Tunnel junctions were grown on (100) GaAs wafers misoriented 2° towards the nearest (111)A plane in a low-pressure horizontal Aixtron MOVPE reactor (AIX-200/4) at 550 °C. The precursors used were TMGa, TMAl, TMIn, AsH_3, PH_3, CBr_4, and DETe diluted in H_2 (200 ppm). The structure of the tunnel junction (Figure 1) consists of an n^{++}-$Ga_{0.51}In_{0.49}P$ cathode (Te doped) with an electrical doping level of $\sim 1.1\times10^{19}$ cm^{-3} and a thickness of 20 nm. The anode is a p^{++}$Al_{0.49}Ga_{0.51}As$ (C doped) layer with an electrical doping level of $\sim 6\times10^{19}$ cm^{-3}, and a thickness of 25 nm. They were grown with a V/III ratio of 24 and 5, respectively. The electrical doping levels were measured in test structures with thicker p-type and n-type layers by using an electrochemical capacitance-voltage profiler. In order to avoid the direct formation of a GaInP/AlGaAs heterojunction in the TJ—which will severely limit the performance of the TJ—the opening of the TMAl source is delayed when switching from the cathode to the anode growth, which implies growing a thin p^{++}GaAs layer (around 3 nm) between both layers. Because this TJ is intended to be placed between the top cell (TC) and the middle cell (MC) in a GaInP/GaInAs/Ge triple junction solar cell (3JSC) lattice matched to Ge, the TJ was grown right after a 20 nm wide GaInP layer (Si doped, doping level 1×10^{18} cm^{-3}). In this way, we analyze if the heterointerface between the MC window layer and the cathode will introduce any kind of series resistance problem in the final 3JSC design. On the contrary, we know from previous analysis [13] that the heterointerface formed between the anode and the TC-BSF will not induce any problem, and hence in the TJ structure no layer mimicking the BSF is included. Needless to say, the successful integration of this tunnel junction in a TJSC needs a careful analysis of the resistive role of all possible heterointerfaces between this TJ and adjacent layers in the real device. Besides, a GaAs cap layer was grown on top of the structure to facilitate the formation of ohmic contacts for the electrical characterization. In order to emulate the thermal load suffered by the TJ during the subsequent growth of the TC in a complete MJSC structure, another identical TJ was grown followed by a thermal annealing at 675 °C for 30 min. Tunnel diodes were fabricated out of as-grown and annealed semiconductor structures with conventional photolithographic techniques. Thermal evaporation of AuGe/Ni/Au and AuZn was used for the formation of the front and back metal contacts, respectively. The chemical etchants used for the mesa formation

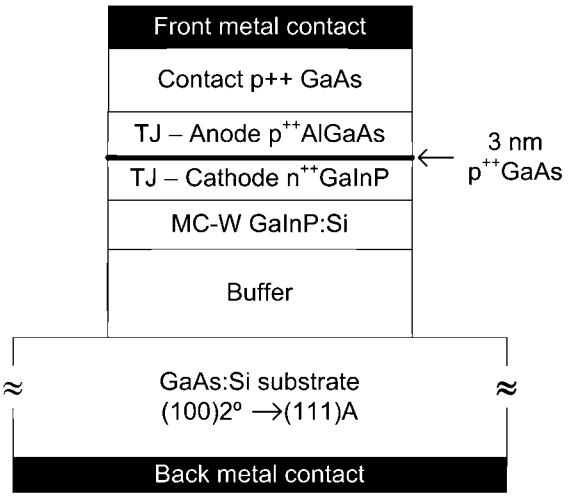

Figure 1. Semiconductor structure of the high bandgap tunnel junction.

were NH_4OH (2:1:10) and HCl for the As-based and P-based semiconductors, respectively.

3. RESULTS AND DISCUSSION

Figure 2(a) shows the J–V curves of the as-grown, circular (5×10^{-5} cm^2) tunnel diodes (black circles). The J–V curves were measured with the four-point probe technique to suppress the influence of the series resistance of the probes and wires on the measurements and were obtained for different TJ devices placed at different positions in the whole wafer area. The peak current density and the equivalent resistance (calculated as the inverse of the slope of the curves at the current density value of 15 A/cm^2) shown in the label in Figure 2, were calculated as the average of the values calculated for each measured curve on different TJs of the same wafer. The average peak current density reaches a value as high as 996 A/cm^2, which is the highest experimental value so far reported for a p^{++}-AlGaAs:C/n^{++}-GaInP:Te tunnel diode designed for III–V multijunction solar cells, while the specific resistance is 7×10^{-5} Ω·cm^2. The value of the specific resistance is of the same order of magnitude as the p^{++}-AlGaAs:C/n^{++}-GaAs:Te TJ presented in [13].

Despite these results, the TJ once introduced in a MJSC architecture will not show such performance due to the aforementioned impact of the thermal load. Indeed, our devices after thermal annealing present a drop in J_p to an average value of 235 A/cm^2 while the equivalent resistance increases to 1.4×10^{-4} Ω·cm^2 (red triangles in Figure 2(a)). Anyway, such peak current would allow the TJ to operate in the ohmic region up to concentrations as high as 15 600 suns ($J_{sc}^{1X} \sim 15$ mA/cm^2), which far exceeds the requirements for ultra-high concentration operation. Besides, the voltage drop corresponding to concentrations of 1000, 5000, and 10 000 suns are of 2, 11, and 26 mV, respectively. Note that these voltage drops are upper limits, because no corrections for voltage drops occurring out of the TJ junction (i.e., metal contacts and substrate resistances) are being considered. In light of these results, this TJ might be also promising for inverted solar cell architectures, where the TJ between the MC and TC suffers even a higher thermal load [5].

Usually, degradation of TJs after thermal annealing has been explained by the following: (i) dopant diffusion that yields junction space charge widening [12,18] and (ii) the formation or evolution of crystal and chemical defects abundant in epilayers doped to degeneracy [19]. We performed secondary ion mass spectroscopy measurements to directly check for Te or C diffusion during thermal annealing. As shown in Figure 3, no diffusion was observed by secondary ion mass spectroscopy within its detection limit (±5% depth error), in agreement with the expected low diffusion coefficients of C and Te. On the other hand, defects have been observed to form in highly Te-doped III–V materials (as the TJ cathode) [13,20], and their formation is probably favored by the low growth temperature used in our TJ. Therefore, changes in the density, structure and properties of the defects or traps associated to high doping concentration might be behind the degradation of J_p after thermal load, as will be discussed in the succeeding text.

Besides, for the TJ presented in this paper, the theoretical values for J_p and r_s predicted with band-to-band tunneling models are several orders of magnitude lower and higher, respectively, than the values empirically obtained [16,21]. This fact, together with the degradation of the J–V characteristic after thermal annealing, suggest the presence of a dominant mechanism—other than band-to-band tunneling—based on traps. In recent years, trap assisted tunneling (TAT) effect has been identified as a key

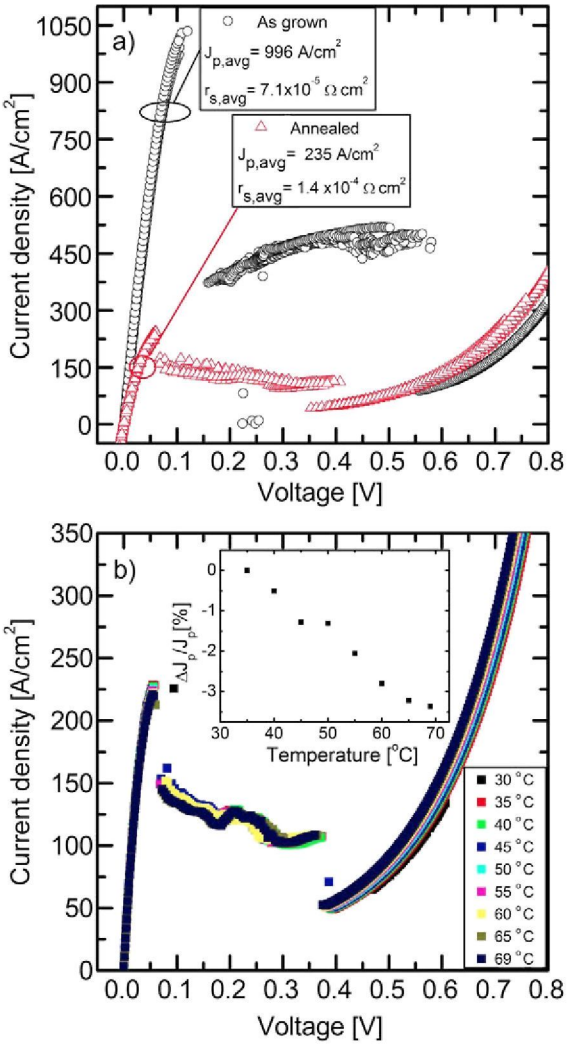

Figure 2. a) J–V measurements of p^{++}-AlGaAs:C/n^{++}-GaInP:Te TJs fabricated with the as-grown structures (black circles) and after thermal annealing at 675 °C for 30 min (red triangles). Measurements for different devices on the same wafer are shown. (b) J–V measurements under temperature of the TJs after thermal annealing. The inset shows the relative difference of J_p with temperature.

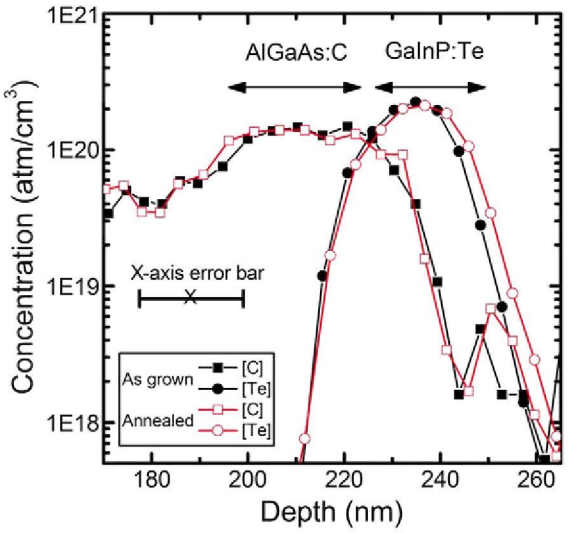

Figure 3. C (squares) and Te (circles) secondary ion mass spectroscopy profiles for the as-grown (filled symbols) and after thermal annealing (open symbols) tunnel junctions structures. The inset shows the error bar of the depth measurement, to facilitate the interpretation of the figure.

contribution to the tunneling current [22]. In this case, the presence of traps (i.e., defects) in the TJ grown is identified by the excess current, generally attributed to tunneling through midgap states [23]. Furthermore, the decrease of the excess current after thermal annealing (as in refs [11,19]) indicates a modification of the properties of these defects, which might also act as traps responsible of TAT effect. However, the exact explanation of the formation and evolution of the sub bandgap defects and their exact role in the TAT process is not completely understood yet. Detailed analysis based of aberration corrected HRTEM of tunnel junction structures is underway to advance in this understanding.

In order to estimate the influence of the TJ properties on the performance of the final solar cell under real working conditions, we measured its J–V curve under typical operation temperatures. A conventional MJSC working in a CPV module under high irradiances and with an ambient T of 30 °C, can reach an equivalent temperature of about 80 °C [24]. Figure 2(b) shows the J–V characteristic of the annealed TJ device at different temperatures in the range of 30–70 °C. J_p shows a slight drop— -3.5% relative at 70°C, see inset of Figure 2(b)—while the equivalent resistance does not experience any significant change with increasing temperature. These small changes in TJ parameters indicate that this design will exhibit the required performance in field operation. In addition, further comments can be made on the evolution of the J–V curves versus temperature. In a conventional TJ, the direct band-to-band tunneling current (i.e., the current density in the TJ related to the tunneling of electrons from the conduction band of the cathode into the valence band of the anode) increases with T [25], as observed for several TJ designs [26,27]. Therefore, the behavior of J_p with T of our high bandgap TJ supports the idea that the dominating tunneling process is other than the direct band-to-band tunneling. On the other hand, the thermal current does show the expected evolution with T, underlining this different behavior of J_p.

As previously commented, optical properties of the TJ are also key for high efficient MJSCs. In the case of MJSCs grown on Ge or GaAs substrates, the p^{++}-AlGaAs:C/n^{++}-GaInP:Te TJ with the J–V curve of Figure 2 is suitable to be placed between the GaInP-based TC and the GaInAs-based MC. In order to estimate the current gain in the MC, in comparison to a more absorbing p^{++}-AlGaAs/n^{++}-GaAs TJ, the following structures were grown. A $Ga_{0.99}In_{0.01}As$ solar cell, similar to the MC of a conventional GaInP/GaInAs/Ge 3JSC, was grown on a Ge(100) substrate. Then the high bandgap TJ was grown on top, followed by a 750 nm GaInP layer that acts here as an optical filter, mimicking the light absorption of a real GaInP-based TC. For comparison, a second structure was grown substituting the high bandgap TJ by a partially absorbing p^{++}-AlGaAs:C/n^{++}-GaAs:Te TJ. As shown in [13], in light of its electrical performance, this TJ design will not limit a MJSC either. This TJ consists of an n^{++}-GaAs cathode (Te doped) with an electrical doping level of $\sim 1 \times 10^{19}$ cm^{-3} and a thickness of 20 nm. The anode is a p^{++}-$Al_{0.49}Ga_{0.51}As$ (C doped) layer with an electrical doping level of $\sim 3 \times 10^{19}$ cm^{-3} and a thickness of 20 nm. The cathode and the anode are sandwiched between AlGaAs barrier layers, as described in [13]. Figure 4 shows the external quantum efficiency (EQE) of these two devices, after the deposition of a MgF_2/ZnS double layer antireflection coating, consisting of 46 nm of ZnS and 100 nm of MgF_2. As can be seen, there is a net increase of the EQE in the MC in comparison to the less-transparent AlGaAs/GaAs TJ. Integrated

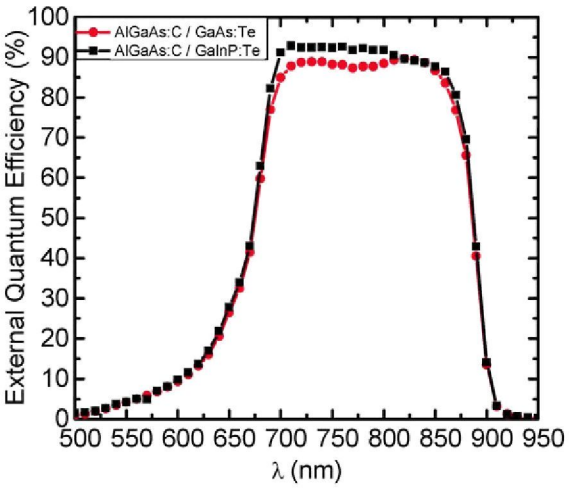

Figure 4. External quantum efficiency measurements of GaInAs SCs with a p^{++}-AlGaAs:C/n^{++}-GaInP:Te (black squares) and a p^{++}-AlGaAs:C/n^{++}-GaAs:Te (red circles) tunnel junctions on top. The results are plotted for devices with ARC.

over the AM 1.5D ASTMG 173-03 (1000 W/m^2) spectrum, this gain is equivalent to an increase in J_{sc} of 0.56 mA/cm^2. Accordingly, our calculations predict an efficiency increase of 1.3% (absolute) at 1000 suns in the final GaInP/GaInAs/Ge triple-junction solar cell, assuming an MC current-limiting MJSC and no modifications of the open circuit voltage or fill factor.

4. CONCLUSIONS

In conclusion, we have developed a highly conductive p^{++}-AlGaAs/n^{++}-GaInP TJ for concentrator MJSC. Regarding the *J–V* characteristics of the TJ after thermal annealing (J_p of 235 A/cm^2 and r_s of 1.4×10^{-4} Ω·cm^2) and its performance under real operating T, this TJ architecture will not electrically limit the MJSC in any practical CPV set-up. The TJ is also transparent for a conventional lattice-matched 3JSC design, yielding a J_{sc} increase of 0.56 mA/cm^2 in the MC with respect to previous and partially absorbing designs. The high values in J_p obtained for the as-grown devices cannot be justified by band-to-band tunneling. Such high J_p values, together with the behavior of the *J–V* curves with T, suggest the presence of an extra dominant tunneling effect based on traps. Experimental and theoretical studies are ongoing to understand the formation of defects in this system and its role in tunneling current enhancement, respectively.

ACKNOWLEDGEMENTS

Financial support from the European Commission and NEDO through the funding of the project NGCPV EUROPE-JAPAN (EU Ref. N: 283798), the Spanish MINECO (TEC2011-28639-C02-01, TEC2012-37286, IPT-2011-1441-920000, IPT-2011-1408-420000) and the Comunidad de Madrid (NUMANCIA II S2009/ENE1477) is gratefully acknowledged. The authors would also like to thank J. Bautista for his continuous technical support and Y. Contreras for the EQE measurements.

REFERENCES

1. Sabnis V, Yuen H, Wiemer M. High-efficiency multijunction solar cells employing dilute nitrides. *In 8th International Conference on Concentrating Photovoltaic Systems*. Toledo, Spain: AIP Conference Proceedings 2012; **1477**(1): 14–19.
2. Guter W, Schöne J, Philipps SP, Steiner M, Siefer G, Wekkeli A, Welser E, Oliva E, Bett AW, Dimroth F. Current-matched triple-junction solar cell reaching 41.1% conversion efficiency under concentrated sunlight. *Applied Physics Letters* 2009; **94**(22): 223504–223504.
3. King RR, Law DC, Edmondson KM, Fetzer CM, Kinsey GS, Yoon H, Sherif RA, Karam NH. 40% efficient metamorphic GaInP/GaInAs/Ge multijunction solar cells. *Applied Physics Letters* 2007; **90**(18): 183516.
4. Chiu P, Wojtczuk S, Zhang X, Harris C, Pulver D, Timmons M. 42.3% Efficient InGaP/GaAs/InGaAs concentrators using bifacial epigrowth, In *Proceedings of the 37th IEEE Photovoltaic Specialists Conference (PVSC)*, Seattle, Washington, USA, 2011; 000771–000774.
5. Geisz JF, Friedman DJ, Ward JS, Duda A, Olavarria WJ, Moriarty TE, Kiehl JT, Romero MJ, Norman AG, Jones KM. 40.8% efficient inverted triple-junction solar cell with two independently metamorphic junctions. *Applied Physics Letters* 2008; **93**(12): 123505–123505.
6. Jones RK, Ermer JH, Fetzer CM, King RR. Evolution of multijunction solar cell technology for concentrating photovoltaics. *Japanese Journal of Applied Physics* 2012; **51**: 10ND01 (4 pages).
7. Algora C, Rey-Stolle I, García I, Galiana B, Baudrit M, Espinet P, Barrigón E, Gonzalez J. III-V multijunction solar cells for ultra-high concentration photovoltaics, In *Proceedings of the 34th IEEE Photovoltaic Specialists Conference (PVSC)*, Philadelphia, USA, 2009; 001571–001575.
8. Sze SM. *Physics of Semiconductor Devices*. Wiley: New York, 1981.
9. Algora C. Very high concentration challenges of III-V multijunction solar cells. In *Concentrator Photovoltaics*. Springer: Heidelberg, Germany, 2007; 89–111.
10. Espinet P, García I, Rey-Stolle I, Algora C, Baudrit M. Extended description of tunnel junctions for distributed modeling of concentrator multi-junction solar cells. *Solar Energy Materials and Solar Cells* 2011; **95**(9): 2693–2697.
11. Jung D, Parker CA, Ramdani J, Bedair SM. AlGaAs/GaInP heterojunction tunnel diode for cascade solar cell application. *Journal of Applied Physics* 1993; **74**(3): 2090–2093.
12. Hayes R, Gibart P, Chevrier J, Wagner S. A stability criterion for tunnel diode interconnect junctions in cascade solar cells. *Solar Cells* 1985; **15**(3): 231–238.
13. García I, Rey-Stolle I, Algora C. Performance analysis of AlGaAs/GaAs tunnel junctions for ultra-high concentration photovoltaics. *Journal of Physics D: Applied Physics* 2012; **45**(4): 045101: (8pp).
14. Mooney P. Deep donor levels (DX centers) in III-V semiconductors. *Journal of Applied Physics* 1990; **67**(3): R1–R26.
15. Yoshida A, Agui T, Katsuya N, Murasawa K, Juso H, Sasaki K, Takamoto T. Development of InGaP/GaAs/InGaAs inverted triple junction solar

cells for concentrator application, In *21st International Photovoltaic Science and Engineering Conference (PVSEC-21)*, Fukuoka, Japan, 2011.

16. Wheeldon JF, Valdivia CE, Walker AW, Kolhatkar G, Jaouad A, Turala A, Riel B, Masson D, Puetz N, Fafard S, Ares R, Aimez V, Hall TJ, Hinzer K. Performance comparison of AlGaAs, GaAs and InGaP tunnel junctions for concentrated multijunction solar cells. *Progress in Photovoltaics* 2011; **19**(4): 442–452.
17. King R, Fetzer C, Colter P, Edmondson K, Ermer J, Cotal H, Yoon H, Stavrides A, Kinsey G, Krut D, Karam N. High-efficiency space and terrestrial multijunction solar cells through bandgap control in cell structures, In *Proceedings of the 29th IEEE Photovoltaic Specialists Conference (PVSC).*, New Orleans, Louisiana, USA, 2002; 776–781.
18. Takamoto T, Yumaguchi M. Mechanism of Zn and Si diffusion from a highly doped tunnel junction for InGaP/GaAs tandem solar. *Journal of Applied Physics* 1999; **85**(3): 1481–1486.
19. Ahmed S, Melloch M. Use of nonstoichiometry to form GaAs tunnel junctions. *Applied Physics Letters* 1997; **71**(25): 3667–3669.
20. Hurle D. Solubility and point defect-dopant interactions in GaAs–I: Tellurium doping. *Journal of Physics and Chemistry of Solids* 1979; **40**(8): 627–637.
21. Hauserm JR, Carlin Z, Bedair SM. Modeling of tunnel junctions for high efficiency solar cells. *Applied Physics Letters* 2010; **97**(4): 042111–042111.
22. Jandieri K, Baranovskii SD, Rubel O, Stolz W, Gebhard F, Guter W, Hermle M, Bett AW. Resonant electron tunneling through defects in GaAs tunnel diodes. *Journal of Applied Physics* 2008; **104**(9): 094506–094506.
23. Chynoweth AG, Feldmann WL, Logan RA. Excess tunnel current in silicon esaki junctions. *Physical Review* 1961; **121**: 684–694.
24. Jaus J, Hue R, Wiesenfahrt M, Peharz G, Bett AW. Thermal management in a passively cooled concentrator photovoltaic module, In *23rd European Photovoltaic Solar Energy Conference and Exhibition*, Valencia, Spain, 2008; 832–836.
25. Esaki L. New Phenomenon in Narrow Germanium p-n Junctions. *Physical Review* 1958; **109**: 603–604.
26. Wheeldon JF, Valdivia CE, Walker A, Kolhatkar G, Hall TJ, Hinzer K, Masson D, Fafard S, Jaouad A, Turala A, Ares R, Aimez V. AlGaAs tunnel junction for high efficiency multi-junction solar cells: Simulation and measurement of temperature-dependent operation, In *Proceedings of the 34th IEEE Photovoltaic Specialists Conference (PVSC)*, Philadelphia, USA, 2009; 000106–000111.
27. Zahraman K, Taylor S, Beaumont B, Grenet J, Gibart P, Verie C. Efficient GaAs tunnel diode as an inter-cell ohmic contact in the tandem AlxGa1-xAs/GaAs, In *Proceedings of the 23th IEEE Photovoltaic Specialists Conference (PVSC)*, Louisville, KY, USA, 1993; 708–711.